Optimization Decomposition for Scheduling and System Configuration in Wireless Networks

Eric Anderson, *Member, IEEE*, Caleb Phillips, *Associate Member, IEEE*, Douglas Sicker, *Senior Member, IEEE*, and Dirk Grunwald, *Member, IEEE, ACM*

***Abstract*—Who gets to use radio spectrum, and when, where, and how?** **Scheduling (who, where, when) and system configuration (how) are fundamental problems in radio communication and wireless networking. Optimization decomposition based on Lagrangian relaxation of signal quality requirements provides a mathematical framework for solving this type of combined problem. This paper demonstrates the technique as a solution to spatial reuse time-division multiple access (STDMA) scheduling with reconfigurable antennas. The joint beam steering and scheduling (JBSS) problem offers both a challenging mathematical structure and significant practical value. We present algorithms for JBSS and describe an implemented system based on these algorithms. We achieve up to 600% of the throughput of TDMA with a mean of 234% in our experiments. The decomposition approach leads to a working distributed protocol producing optimal solutions in an amount of time that is *at worst* linear in the size of the input. This is, to the best of our knowledge, the first actually implemented wireless scheduling system based on dual decomposition. We identify and briefly address some of the challenges that arise in taking such a system from theory to reality.**

***Index Terms*—Antenna arrays, cross-layer design, directional antennas, distributed algorithms, optimal scheduling, optimization, packet radio networks, radio communication, time-division multiple access, wireless mesh networks, wireless networks.**

I. Introduction

THIS paper demonstrates a novel approach to minimizing interference and maximizing spatial reuse for competing spectrum users. These concerns are significant any time interference is a limiting factor, for example in packet radio networking, mobile telephony, and radio repeaters. Here, we specifically consider explicitly scheduled medium access control (MAC) protocols such as time-division multiple access (TDMA). These MACs enable optimizations for spatial reuse and avoid problems that random-access carrier-sense protocols (e.g., CSMA/CA) incur when deployed in large networks where hidden terminal effects limit performance.

Manuscript received October 18, 2011; revised April 10, 2012; August 24, 2012; and December 28, 2012; accepted February 13, 2013; approved by IEEE/ACM TRANSACTIONS ON NETWORKING Editor E. Modiano. Date of publication December 16, 2013; date of current version February 12, 2014.

E. Anderson is with the Department of Electrical and Computer Engineering, Carnegie Mellon University, Pittsburgh, PA 15213 USA (e-mail: andersoe@ece.cmu.edu).

C. Phillips, D. Sicker, and D. Grunwald are with the Department of Computer Science, University of Colorado, Boulder, CO 80309 USA (e-mail: cphillips@smallwhitecube.com; sicker@colorado.edu; grunwald@colorado.edu).

Color versions of one or more of the figures in this paper are available online at http://ieeexplore.ieee.org.

Digital Object Identifier 10.1109/TNET.2013.2289980

We present a joint optimization process for scheduling and physical-layer configuration that achieves greater spatial reuse than solving the two problems separately. Without integration, a "chicken-and-egg" problem exists: If PHY decisions are made before scheduling, they cannot be optimized for the communication that actually occurs. If scheduling decisions are made first, the scheduler cannot know what the actual radio properties of the network will be.

The joint approach produces significant gains for scheduling and antenna reconfiguration. An analysis of the performance of our algorithm in simulation shows a mean speedup relative to simple TDMA of 234% with as much as 600% improvement in some scenarios. We also show that simple techniques such as greedy approaches to antenna steering and scheduling result in substantial interference between neighboring links.

A. Combined Scheduling and System Configuration

We define *scheduling* as assigning users (either transmitters or links) to discrete slots of time in which they may generate radio signals. In general, this is a many-to-many mapping. We define *system configuration* as stipulating the way in which users access the RF spectrum in each time-slot. Each user's transmit power, channel, modulation scheme, and antenna configuration are examples of system configuration variables. These assignments are upper bounds on how users affect each other.

The combined problem is interesting when the optimal (or feasible) configuration depends on the schedule *and vice-versa*, so that neither problem can be solved independently. We tackle this by: 1) defining a joint optimization problem that captures the effects and constraints of both MAC- and PHY-layer decisions but is impractical to solve directly; and 2) decomposing this into a form that is practically solvable.

B. Spatial-Reuse TDMA With Configurable Antennas

Fig. 1 illustrates the pitfalls of treating scheduling and antenna configuration separately. With naïve configuration 1, potential interference paths get the same antenna gain as intended signal, so both links cannot be scheduled together with any reasonable signal-to-interference-plus-noise ratio (SINR). A configuration such as 1 attenuates the interference, allowing both links to operate. This case will occur only if the antenna patterns and schedule are chosen jointly—a scheduling-oblivious antenna choice 1 makes this schedule impossible, and (in the presence of other possible links and interference) there is no

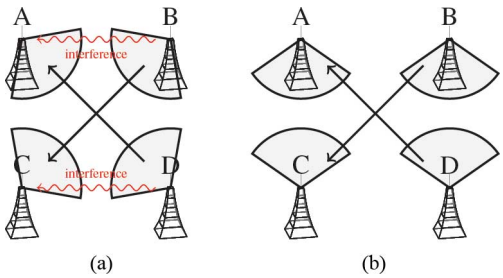

Fig. 1. Example: Links B to C and D to A can be scheduled concurrently, but not with greedy antenna configurations. (a) Greedy antenna configuration: Nodes have their beam pattern main lobes pointed directly at their communicating partner. (b) Scheduling-aware antenna configuration: Beam patterns reduce interference *to enable* a denser schedule.

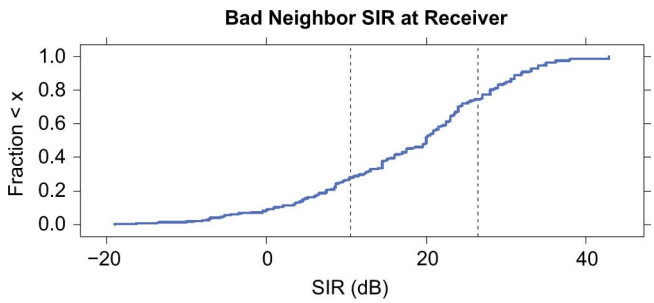

Fig. 2. Empirical cumulative distribution function (ECDF) of interference between neighboring links when greedy antenna patterns are used. Reference lines show theoretical SNR values for 10^{-6} BER with BPSK (10.5 dB) and 64-QAM (26.5 dB) modulation schemes.

reason for these better antenna patterns to be chosen unless this schedule is being considered.

To quantify the prevalence of this situation in a real network, we conducted an empirical study using the WART wide-area phased array testbed [1]. Considering all feasible two-link transmission sets with each link using its independent best (greedy) antenna patterns, we find significant interlink interference. The distribution of signal-to-interference ratios (SIRs) is shown in Fig. 2. The reference lines mark 10.5 and 26.5 dB, which are theoretical signal-to-noise ratio (SNR) thresholds[1] to achieve a bit error rate (BER) of 10^{-6} using two common modulation schemes, BPSK and 64 QAM [2]. Pairwise interference is sufficient to preclude BPSK and 64 QAM at this BER in 28% and 74% of cases, respectively.

This problem motivates our integrated approach: We define a joint problem and then decompose it into subproblems that are coupled by a Lagrange multiplier that functions as a marginal *value* or *price of signal quality* for each user. This is the model shown in Fig. 3.

The intuition behind this approach is simple: A high signal quality price for a given link indicates to the scheduling process that it is difficult to satisfy that link's SINR requirements, and it might be better to not schedule that link in this time-slot. The same high price indicates to the configuration process that the link's signal quality is limiting the overall utility and it would

[1]These SNR thresholds are roughly comparable to SIR numbers if the interfering signal is close to Gaussian noise and other sources of noise and interference are negligible.

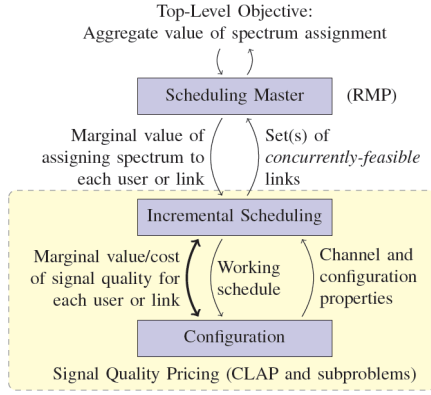

Fig. 3. Problem decomposition model: The lower block shows the decomposition by signal quality pricing.

be good to improve it. By iteratively solving the scheduling and configuration problems, updating the price each time, the system converges to a joint solution.

In Section II, we discuss background and related work. In Section III, we present our formulation along with a series of decompositions which transform this problem into a tractable form. Section IV evaluates this algorithm via numerical experiments, showing that optimal solutions are both achieved quickly and offer substantial speedup over (non-spatial-reuse) TDMA schedules. In Section V, we discuss a testbed proof-of-concept implementation of our approach, and finally in Section VI, we summarize our contributions and conclude.

II. Related Work

There are two main areas of closely related work that bear discussing: optimization-based wireless scheduling and wireless networking with directional antennas. At the intersection of the two, there are several proposals that consider antennas in the context of scheduling, but none that do so with significant integration or optimality results. A more comprehensive discussion is given in [3, Sec. 2]; see especially Section 2.2 for models of interference and Section 2.8 for optimization decomposition in wireless networking.

A. Optimization and Wireless Scheduling

There is a significant body of theoretical work in the area of optimization and wireless scheduling, although ours is one of the first to produce an implementation. We identify a few salient examples here. The principle optimization foundations were laid by Arikan's formulation of $\vec{f}$-feasibility and Toumpis and Goldsmith's analysis of capacity regions [4], [5]. The first explicit treatment of utility maximization and its dual problems in networking is Kelly's work on rate control [6]. Björklund *et al.* introduced the first optimization formulation of wireless scheduling of which we are aware [7]. The authors present a linear column generation formulation. The paper compares the complexity and efficacy of scheduling by link and by node (transmitter), reestablishes NP-completeness results for both problems, and compares an integer formulation to its continuous relaxation. Björklund's formulation is the starting point for the present paper.

Xiao *et al.* present the Simultaneous Routing and Resource Allocation (SRRA) problem, which is a joint optimization approach to routing and something similar to scheduling [8]. The authors make, and acknowledge, the assumption that link capacities can be determined completely by sender-local decisions. While this abstracted view does not correspond with any real system, it enables a very clean and logical development of techniques central to multilayer optimization in networks. This paper presents hierarchical dual decomposition using subgradient solution methods and the coupling of routing and scheduling by per-node capacity prices.

The general principles of the preceding works are further explored in a series of papers by Chiang *et al.* under the moniker of "layering as optimization decomposition" [9]–[11]. These address wireless scheduling specifically and develop the broader notion of network layers as *computational elements* coupled together to solve some global objective. Of particular import for scheduling is work by Tan *et al.*, which shows that many nonconvex functions of interest, such as interference-limited Shannon capacity, are convex when transferred to the logarithmic domain, and therefore admit equivalent convex formulations [12]–[14]. A log change of variables for this present work is explored in [3].

Several abstractions of interference (e.g., pairwise node or link conflicts/clique constraints, especially one- or two-hop models) enable efficient scheduling algorithms [15], [16]. Such abstractions do not translate well to the joint scheduling and antenna selection problem because the "neighbor" relation between any two nodes depends strongly on the antennas.

B. Power Control

There is a substantial body of work on power control in wireless networks, especially cellular systems. This problem is fundamentally different from antenna selection because of its intrinsic regularity: Changing a station's transmit power by a factor k changes the received signal (or interference) at every other station by exactly k. This regularity does not exist for antenna configuration—the value of a directional antenna is precisely that it increases gain toward some stations while reducing the gain toward others. Techniques for power control do not *directly* translate to antenna selection, but recent work in that area has produced some sophisticated analysis that may be applicable. In particular, efficient power control algorithms with bounded approximation ratios are presented in [14] and [17]. Additionally, Tan *et al.* introduce Lagrange multipliers on SINR constraints as an "interference price" to balance power allocation between interfering links [12], [13].

C. Scheduling With Antenna Considerations

The remaining related works can be divided into two groups: those that do not consider antenna configuration directly, and those that consider it, but separately from scheduling.

The first group assumes idealized effects of using directional antennas, rather than the actual RF gains of specific antenna configurations. Such approaches are computationally easier, but the assumptions are often incorrect. Cain *et al.* assume that an arbitrarily narrow beamwidth allows interference to be disregarded entirely and propose scheduling based on only a simplex/unicast constraint [18]. Several other papers assume a "pie wedge" region of interference [19], [20]. Sundaresan *et al.* consider real signal strength and interference, but assume that a smart antenna can completely eliminate interference from a given number of stations. Scheduling is then as with fixed antennas, but with the addition of choosing a set of interferers to disregard [21]. Sundaresan's work is conceptually the closest work to the problem we are addressing, but its assumptions are typically false: A K-element phased-array antenna has $K-1$ "degrees of freedom," but they are not arbitrary. The signal strength can only be varied independently in $K-1$ directions if they correspond to mutually orthogonal antenna vectors, which is in general not the case [22, Sec. 10.1]. All of the preceding papers are based on simplifying assumptions that do not hold well in practice.

The second group of papers considers actual antenna and radio effects, but with the configuration determined separately from scheduling, as in the example in Fig. 1(a). A series of papers by Sánchez-Garache and Dyberg investigates scheduling with the assumption that the stations in every link beamform toward each other [23], [24].

Recent work by Liu *et al.* considers partial integration of antenna selection and scheduling using a conflict graph model based on pairwise interference [25], [26]. This simplification leads to a significant loss of optimality, but enables simple and efficiently implementable protocols. Jorswieck *et al.* present an analytical characterization of the potential benefit of beamforming in a given group of concurrent users based on their channel correlation properties, but do not propose any scheduling process to take advantage of this [27].

Our proposed technique has two properties that we consider important and that are lacking in the existing approaches: 1) The effects of an antenna configuration can be arbitrary and measured *in situ*. Nothing about the algorithm depends on an *a priori* model of what gains antenna configuration will achieve.[2] 2) Optimal schedules can be found even when they depend on a specific antenna configuration *and* that antenna configuration would not otherwise be chosen. That is, all the prior approaches suffer from some form of the "chicken-and-egg" problem described in the Introduction.

III. Model and Algorithms

In this section, we describe a distributed and decomposed mathematical solution to the integrated beam steering and scheduling problem. We begin with a formalization of the objective and constraints. We then present a series of decompositions to make the problem more computationally tractable. For clarity, proofs have been omitted from the main body of the text and given in the Appendix.

Notation: Variables and constants are vectors or matrices except where otherwise noted; vectors are regarded as column vectors. Indexing is indicated with subscripts. An undecorated variable is a decision variable in the problem at hand, while a bar (e.g., $\bar{S}$) indicates an estimate, especially one that is treated as a constant. This arises when subproblems take turns solving for

[2]We will assume that (the effect of) a node's antenna configuration can be described as a set of gains toward other nodes. Even this assumption is imperfect, but it is much milder than the others discussed here.

TABLE I
NOTATION

Symbol	Interpretation
A	The set of all links
N	The set of all nodes
L_A	The set of all concurrently-feasible link sets
L_A^t	The generated subset of L_A at time t
x_l	Number of slots assigned to link set $l \in L_A$
q_{ij}	Demand (in slots) for link ij
S_{ij}	Activation of link ij (in current link set)
M_{ij}	Max. non-signal power s.t. (16) holds when $S_{ij} = 0$
V_i	Node i is active (in current link set)
P_i	Transmit power of node i
γ_1	Desired SINR threshold
N_r	Receiver noise level
D_{ij}	Directivity of node i in the direction of node j
$Lb(i,j)$	Path loss from node i to node j
G_{ikp}	Gain for node i using pattern p, toward node k
B_{jp}	Beam (antenna, pattern, ...) p used at node j

the best values for "their" variables, taking the values of other variables as given. The hat (e.g., $\hat{S}$) indicates the estimates used in primal solution extraction. The meanings of repeatedly used symbols are given in Table I. Many symbols are indexed by the link set l, but outside of the master problems JBSS-MP and RMP, only one link set is considered at a time, so l is omitted for simplicity.

A. Formulation

A direct statement of the integrated scheduling and antenna configuration process is given in (JBSS-MP) as follows:

[JBSS-MP]

$$\min_{x_l} \sum_{l \in L_A} x_l \tag{1}$$

$$\text{s.t.} \sum_{l \in L_A} S_{ijl} x_l \geq q_{ij} \qquad \forall_{i,j} \tag{2}$$

$$\sum_{j:(i,j)\in A} S_{ijl} + \sum_{j:(j,i)\in A} S_{jil} \leq 1 \qquad \forall_{i,l} \tag{3}$$

$$\left.\begin{array}{l} \frac{P_{il} D_{ijl} D_{jil}}{Lb(i,j) N_r} S_{ijl} + \gamma_1 (1 + M_{ijl})(1 - S_{ijl}) \\ \quad \geq \gamma_1 \left(1 + \sum_{k \in N \setminus \{i,j\}} \frac{P_{kl} D_{kjl} D_{jkl}}{Lb(k,j) N_r} V_{kl}\right) \end{array}\right\} \quad \forall_{i,j,l} \tag{4}$$

$$S_{ijl} \leq V_{il} \qquad \forall_{i,j,l} \tag{5}$$

$$\sum_{p \in P} B_{jpl} = 1 \qquad \forall_{j,l} \tag{6}$$

$$D_{ik} = \sum_{p \in P} G_{ikp} B_{ipl} \qquad \forall_{i,k,l} \tag{7}$$

$$x_l \geq 0 \qquad \forall_{l \in L_A} \tag{8}$$

$$S_{ijl},\ B_{jpl} \in \{0, 1\}. \tag{9}$$

The objective, (1), is to minimize the time allocated to all link sets. For each link set l in the universe of possible concurrent link sets L_A, x_l indicates the time for which l is active. We overload l to also denote an index referring to the link set. Constraint (2) requires that the total time for which link sets containing each ij are activated is sufficient. S_{ijl} is a Boolean variable indicating whether link ij is active in link set l, and q_{ij} is the demand for link ij, measured in time. Constraint (3) specifies that in any given link set l, every node j may be active in *at most* one link. This precludes duplex operation, as well as transmitting to or receiving from multiple partners.

Constraint (4) specifies that minimum SINR requirements are met, taking antenna configuration into account. The formulation of this constraint is patterned after Björklund and can be somewhat unintuitive. See [28, Ch. 3, Eq. (3.12), and Appendix B]. Ignoring the second term, it specifies that if the link ij is used, the received signal strength must exceed the combined interference and noise level at j by factor γ_1. The first term is a product of 0–1 variable S_{ijl}, and the second term is a product of $(1 - S_{ijl})$. The second term ensures that the constraint is satisfied when $S_{ijl} = 0$: The constraint is effectively a no-op when the link ij is not selected. For any given ij, when $S_{ijl} = 1$, the constraint reduces to the following inequality:

$$\frac{P_i D_{ij} D_{ji}}{Lb(i,j) N_r} S_{ij} \geq \gamma_1 \left(1 + \sum_{k \in N \setminus \{i,j\}} \frac{P_k D_{kj} D_{jk}}{Lb(k,j) N_r} V_k\right). \tag{10}$$

Considering a given link set l, the subscripts can be removed for clarity.

The left-hand side gives the received SNR in linear units. The right-hand side is the sum of the contribution above the noise floor of received interfering signals plus 1. The 0–1 variable V_k specifies that node k is (or may be) transmitting in the given time-slot.

This formulation is quite general in terms of how the antenna effects are modeled: For each node, its antenna gain toward any other node can be an arbitrary function of its selected configuration. That is, for any given nodes i and k, the gain with one configuration (G_{ikp_1}) in no way constrains the gain with another (G_{ikp_2}), and similarly for any given configuration p, the gain toward one node (G_{ik_1p}) in no way constrains the gain toward any other (G_{ik_2p}). This is important because it means that the algorithm can use the *actual measured effects* of a configuration choice, however irregular they may be. Even so, there is an important limitation: Calculating the received signal strength as $\frac{P_i D_{ij} D_{ji}}{Lb(i,j)}$ assumes that effects of the transmitter's antenna gain, the receiver's antenna gain, and the path loss are orthogonal. While this model is almost universally accepted, it has been shown that this does not always hold for directional antennas [29]: A directional antenna does not simply strengthen or attenuate the signal, but in effect selects a *view* of the environment and the other antennas, such that the combined effect is a more complicated function of the environment and all the antenna configurations. We measured the error arising from this assumption on the WART testbed and the ECDF over all possible links and antenna configuration in the testbed is shown in Fig. 4. The error is roughly normally distributed with mean 0 and standard error 5.4 dB, relative to a total antenna selection effect of ≈ 35 dB. Despite this error, we continue to model the antenna effects and path loss as orthogonal components of signal strength for computational simplicity: Without assuming *some* structure, the problem becomes irreducibly combinatorial.

Constraint (5) couples the decision variables S_{ijl} and V_{il} so that if any link ij is selected, the variable V_{il} reflects that i is

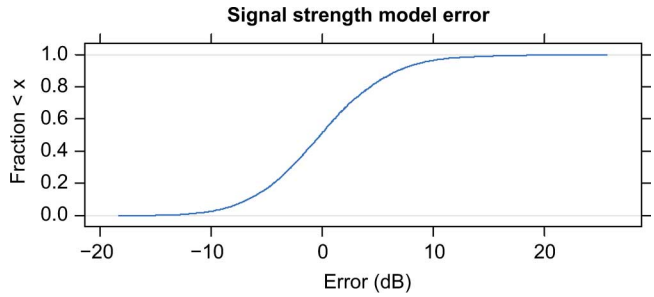

Fig. 4. ECDF of orthogonal path loss and antenna gain model on WART data.

transmitting. The 0–1 variable B encodes the antenna configuration (beam pattern) used at each node: B_{jpl} indicates whether node j uses beam pattern p in link set l. Constraint (6) specifies that each node must select a convex combination of its beam patterns; when $B_{jpl} \in \{0,1\}$, the only way to satisfy this is to choose exactly one pattern. Constraint (7) connects the directional gain variables D_{ikl} to the choice of antenna beam B_{ipl}. Constraints (8) and (9) specify positivity and 0–1 requirements for variables. Minor variations on constraints (6) and (2) generalize this problem to include forms of rate selection and power control [30].

B. Computational Complexity

The master problem (JBSS-MP) is complete, but a direct solution is computationally intractable. The program is mixed-integer cubic, meaning that the objective or constraints involve polynomials of degree 3 and a mixture of continuous and integer variables. There are a number of efficient algorithms for solving linear and quadratic programs, but cubic programs are as difficult as arbitrary nonlinear programs. There is no obvious way to reformulate the cubic terms ($D_{ijl}D_{jil}S_{ijl}$ and $D_{kjl}D_{jkl}V_{kl}$) away, as they are the fundamental determinants of SINR and are all real decision variables. The problem is also vast. The subscript l indexes the set of all possible sets of links L_A, having dimension 2^m for m links. Several of the variables are indexed over $L_A \times N \times N$, meaning there are $\Theta(n^2 2^m)$ variables and similarly many constraints.

C. Decompositions

Our first decomposition is aimed at pruning the overall search space: Rather than considering every subset of the set of links from the outset, we incrementally build up the problem by searching for "promising" sets of links to consider. This is *delayed column generation* or *implicit enumeration*, based on *Danzig–Wolfe decomposition*. This decomposition is used in many previous scheduling works, including [7], [8], [31], and [32]. The objective function of JBSS-MP is simple; the complexity lies in defining the region of feasible values. Any set of feasible points defines a convex hull that is a subset of the feasible region. Therefore, given any such set of feasible points, the original problem can be replaced with a *restricted master problem* (RMP), in which the only constraint is that the solution must lie within the polytope defined by those points. For a simple objective function and any modest number of points, the RMP is a computationally simple conservative approximation of the full master problem. The quality of the approximation depends on how closely this polytope approximates the true feasible region in the area of the master problem's optimal solution. Implicit enumeration proceeds by iteratively solving the RMP and a subproblem that searches for additional *objective-improving* feasible points to extend the polytope. If no such points exist, then the approximating polytope matches the true constraint region *at the optimal point*, and therefore the solution to the RMP is the optimal solution to the master problem.

Applying this decomposition to JBSS-MP produces the RMP and a subproblem that we designate the Configuration and Link Activation Problem (CLAP). The time allocated to each feasible point l is denoted x_l, and the activation level of each link i, j in each l—an output of the subproblem, not a decision variable in RMP—is denoted $\bar{S}_{ijl}$. The set of feasible points defining the RMP's approximation polytope in iteration t is L_A^t. For any known set of feasible points L_A, assigning time to such sets is a convex (in fact linear) problem

[RMP]

$$\min_{x_l} \quad \sum_{l \in L_A^t} x_l \tag{11}$$

$$\text{s.t.} \quad \sum_{l \in L_A^t} \bar{S}_{ijl} x_l \geq q_{ij} \qquad \forall_{ij} \tag{12}$$

$$x_l \geq 0 \qquad \forall_{l \in L_A^t}. \tag{13}$$

Solving RMP produces not only a primal solution $X^*_{\mathrm{RMP}_t}$, but also dual costs for the constraints (12), $\bar{\beta}_{ij}$. These are inputs to the subproblem CLAP, which tries to "loosen" the most limiting capacity constraints (indicated by $\bar{\beta}$) by producing a set of concurrently feasible links indicated by S and associated antenna gains and configurations D and B. In the context of Fig. 3, CLAP is *incremental scheduling* and *configuration* and RMP is the *scheduling master*

[CLAP]

$$\max_{S} \quad \bar{\beta}^T S \tag{14}$$

$$\text{s.t.} \quad \sum_{j:(i,j)\in A} S_{ij} + \sum_{j:(j,i)\in A} S_{ji} \leq 1 \qquad \forall_i \tag{15}$$

$$\left.\begin{array}{l} \frac{P_i D_{ij} D_{ji}}{Lb(i,j) N_r} S_{ij} + \gamma_1 (1 + M_{ij})(1 - S_{ij}) \\ \quad \geq \gamma_1 \left(1 + \sum_{k \in N \setminus \{i,j\}} \frac{P_k D_{kj} D_{jk}}{Lb(k,j) N_r} V_k\right) \end{array}\right\} \quad \forall_{i,j} \tag{16}$$

$$S_{ij} \leq V_i \qquad \forall_i \tag{17}$$

$$D_{ik} = \sum_{p \in P} G_{ikp} B_{ip} \qquad \forall_{i,k} \tag{18}$$

$$\sum_{p \in P} B_{jp} = 1 \qquad \forall_j \tag{19}$$

$$S_{ij},\ B_{jp} \in \{0,1\}. \tag{20}$$

The remaining decompositions serve to break a single large problem into many small ones. When the complexity of solving a problem is superlinear (and potentially exponential) in the size of the problem, solving k problems of size n/k is more appealing than solving one problem of size n. A problem that can be so subdivided is called *separable*, and our goal is to create

such a structure. As CLAP is not truly separable, we apply Lagrangian relaxation to "get rid of" the constraints that bind the almost-separable components together. This simplified problem (the relaxed primal problem) will be much easier to solve, but the complicating constraints are not gone: The subproblems of the relaxed primal problem will be coupled together by *Lagrange multipliers*, and the Lagrangian dual problem is to find values for those multipliers such that the "removed" constraints are still satisfied.

The problem RMP is trivial, but CLAP retains most of the original complexity of JBSS-MP. Crucially, however, it is no longer dimensioned over the set of all possible sets of links: For n nodes, the number of variables and constraints are both $\Theta(n^2)$. The primary computational difficulty in CLAP comes from constraint (16), which is order 3 and mixed-integer. Let us define vector-valued convenience function $d^s(\cdot)$, giving the degree of violation of constraint (16). Entry ij is given by

$$d^s(S,D,V)_{ij} = -\left(\frac{P_i D_{ij} D_{ji}}{Lb(i,j)N_r} S_{ij} + \gamma_1(1+M_{ij})(1-S_{ij}) - \gamma_1\left(1 + \sum_{k\in N\setminus\{i,j\}} \frac{P_k D_{kj} D_{kj}}{Lb(k,j)N_r} V_k\right)\right). \quad (21)$$

Define a Lagrangian with regard to (14) and (16) as

$$\mathcal{L}(S,\lambda) = \bar{\beta}^T S - \lambda^T d^s(S,D,V). \quad (22)$$

This gives a dual function

$$\phi(\lambda) = \max_{S,D,V} \mathcal{L}(S,D,V,\lambda). \quad (23)$$

The corresponding Lagrangian dual problem is CLAP-dual-1. The resulting Lagrangian relaxed primal problem (RPP) of CLAP is given as follows:

[CLAP-dual-1]

$$\begin{aligned} \min_{\lambda} \quad & \phi(\lambda) \\ \text{s.t.} \quad & \sum_{j:(i,j)\in A} S_{ij} + \sum_{j:(j,i)\in A} S_{ji} \le 1 \qquad \forall_i \\ & S_{ij} \le V_i \qquad \forall_i \\ & D_{ik} = \sum_{p\in P} G_{ikp} B_{ip} \qquad \forall_{i,k} \\ & \sum_{p\in P} B_{jp} = 1 \qquad \forall_j \\ & S_{ij},\ B_{jp} \in \{0,1\} \qquad \forall i,j,p \end{aligned} \quad (24)$$

$$\begin{aligned} \max_{S,D,V} \quad & \bar{\beta}^T S + \bar{\lambda}^T d^s(S,D,V) \\ \text{s.t.} \quad & \text{constraints (15)–(19)} \\ & \textbf{except (16)} \end{aligned} \quad (25)$$

where $\bar{\lambda}$ denotes an *estimate* of the optimal multipliers λ^*. This transformation introduces a possible duality gap; in most but not all cases, this gap is found to be zero.

This RPP is block-structured and separable into two subproblems coupled by the Lagrange multipliers λ. These problems correspond to the *Incremental Scheduling* and *Configuration* tasks in Fig. 3. We label these the Fixed-antenna Link Activation Problem (FLAP) and the Fixed-link Antenna Reconfiguration Problem (FARP). FLAP takes estimated Lagrange multipliers and antenna gains $\bar{\lambda}$, $\bar{D}$ as parameters and computes link activations S. Conversely, FARP takes $\bar{\lambda}$ and estimated $\bar{S}$ as parameters and computes D

[FLAP]

$$\begin{aligned} \max_{S,V} \quad & \left\{ \bar{\beta}^T S - \sum_{ij} \bar{\lambda}_{ij} \left(\frac{P_i \bar{D}_{ij} \bar{D}_{ji}}{Lb(i,j)N_r} S_{ij} + \gamma_1(1+M_{ij})(1-S_{ij}) - \gamma_1\left(1 + \sum_{k\in N\setminus\{i,j\}} \frac{P_k \bar{D}_{kj} \bar{D}_{kj}}{Lb(k,j)N_r} V_k\right)\right)\right. \\ \text{s.t.} \quad & \sum_{j:(i,j)\in A} S_{ij} + \sum_{j:(j,i)\in A} S_{ij} \le 1 \qquad \forall_i \\ & S_{ij} \le V_i \qquad \forall_{i,j} \\ & S_{ij} \in 0,1 \qquad \forall i,j. \end{aligned}$$

This subproblem has the integrality property, so the constraint $S_{ij} \in \{0,1\}\ \forall i,j$ can be dropped. This in turn allows it to be solved using more efficient continuous methods, without incurring an integrality gap.

Proposition 3.1: The continuous relaxation of FLAP is equivalent to FLAP with integer S

[FARP]

$$\begin{aligned} \max_{D,B} \quad & \left\{ \bar{\beta}^T \bar{S} - \sum_{ij} \bar{\lambda}_{ij} \left(\frac{P_i D_{ij} D_{ji}}{Lb(i,j)N_r} \bar{S}_{ij} + \gamma_1(1+M_{ij})(1-\bar{S}_{ij}) - \gamma_1\left(1 + \sum_{k\in N\setminus\{i,j\}} \frac{P_k D_{kj} D_{kj}}{Lb(k,j)N_r} \bar{V}_k\right)\right)\right. \\ \text{s.t.} \quad & D_{ik} - \sum_{p\in P} G_{ikp} B_{ip} = 0 \qquad \forall_{i,k} \\ & \sum_{p\in P} B_{ip} = 1 \qquad \forall_i. \end{aligned}$$

Note that $\bar{\beta}^T \bar{S}$ is a constant and is dropped for simplicity in subsequent formulations. The constraints are easily separable by index i. The objective function is also separable with the following change of variables. Let x denote the vector of all antenna gains D. Now let i partition x as: $x_i = \cup_{k\neq i} \{D_{ik}\}$

$$g_i(x) = \begin{cases} \sum_j \left(\frac{1}{2} \bar{\lambda}_{ij} \bar{S}_{ij} \frac{P_i}{Lb(i,j)N_r} D_{ij} \bar{D}_{ji} \right) + \frac{k}{|N|}, \\ \quad \text{if } i \text{ is a transmitter} \\ \sum_j \left(\frac{1}{2} \bar{\lambda}_{ji} \bar{S}_{ji} \frac{P_j}{Lb(j,i)N_r} \bar{D}_{ji} D_{ij} \right) + \frac{k}{|N|}, \\ \quad \text{if } i \text{ is a receiver} \end{cases}$$

$$h_i(x) = \begin{cases} \sum_j \left(\sum_{k,l\in N\setminus\{i,j\}} \left(\frac{1}{2} \gamma_1 \bar{S}_{ij} \bar{\lambda}_{kl} \frac{P_i}{Lb(i,l)N_r} D_{il} \bar{D}_{li} \right) \right) \\ \quad \text{if } i \text{ is a transmitter} \\ \sum_j \left(\sum_{k,l\in N\setminus\{i,j\}} \left(\frac{1}{2} \gamma_1 \bar{S}_{ji} \bar{\lambda}_{ji} \frac{P_k}{Lb(k,i)N_r} \bar{D}_{ki} D_{ik} \right) \right) \\ \quad \text{if } i \text{ is a receiver} \end{cases}$$

$$f_i(x) = g_i(x_i) - h_i(x)$$

$$f(x) = \sum_i f_i(x) \text{ given } \sum_j \bar{S}_{ij} \le V_i \qquad \forall_i.$$

Now, $1 - f(x)$ is equivalent to the FARP objective and is clearly separable by index i. Using this separation, we define an instance of the Single Node Antenna Reconfiguration Problem (SNARP) for every node in the network

$[\mathrm{SNARP}_i]$

$$\max_{D,B} \quad 1 - f_i(D) \tag{26a}$$

$$\text{s.t.} \quad D_{ik} - \sum_{p \in P} G_{ikp} B_{ip} = 0 \qquad \forall_k \tag{26b}$$

$$\sum_{p \in P} B_{ip} = 1 \tag{26c}$$

$$B_{ip} \leq 1 \qquad \forall_{p \in P} \tag{26d}$$

$$B_{ip} \geq 0 \qquad \forall_{p \in P}. \tag{26e}$$

Proposition 3.2: SNARP_i with continuous variables has an optimal solution equal to that with Boolean B_{ip}.

In the interest of scalability, it would be desirable to similarly separate FLAP. Unfortunately, the duplex constraint prevents this and is not easily massaged away algebraically. To address this, we extend the Lagrangian relaxation of CLAP to the constraint $\sum_{j:(i,j)\in A} S_{ij} + \sum_{j:(j,i)\in A} S_{ji} \leq 1 \, \forall_i$. Paralleling (21), we define a convenience function that quantifies the violation of that constraint: Let $d^d(S)$ be the function having the ith element given by

$$d^d(S)_i = \sum_{j:(i,j)\in A} S_{ij} + \sum_{j:(j,i)\in A} S_{ji} - 1. \tag{27}$$

Now, let us also define a function $d'^s(S, V)$ to be $d^s(S, D, V)$ where the antenna gain variables D are replaced with fixed estimates $\bar{D}$.

These two definitions allow us to cleanly state a Lagrangian dual problem that will be easy to separate both *vertically* into scheduling and antenna configuration components and *horizontally* into symmetrical per-node components.

Let us define a new Lagrangian function $\mathcal{L}'(\cdot)$ as follows:

$$\mathcal{L}'(S, D, V, \lambda, \mu) = \bar{\beta}^T S - \lambda^T d^s(S, D, V) - \mu^T d^d(S). \tag{28}$$

This gives a new dual function $\phi'(\lambda, \mu)$ as follows and corresponding problem dual problem CLAP-dual-2:

$$\phi'(\lambda, \mu) = \max_{S,D,V} \mathcal{L}'(S, D, V, \lambda, \mu)$$

[CLAP-dual-2]

$$\min_{\lambda,\mu} \quad \phi'(\lambda, \mu)$$

$$\text{s.t.} \quad S_{ij} \leq V_i \qquad \forall_i$$

$$D_{ik} = \sum_{p \in P} G_{ikp} B_{ip} \qquad \forall_{i,k}$$

$$\sum_{p \in P} B_{jp} = 1 \qquad \forall_j. \tag{29}$$

This produces a new relaxed primal version of FLAP, RP-FLAP. FARP remains unchanged. Now, both subproblems (RP-FLAP for link activation and FARP for antenna configuration) can be broken into independent per-node components

[RP-FLAP]

$$\max_{S,V} \quad \bar{\beta}^T S + \bar{\lambda}^T d'^s(S, V) - \bar{\mu}^T d^d(S)$$

$$\text{s.t.} \quad S_{ij} \leq V_i \qquad \forall_{ij}. \tag{30}$$

RP-FLAP is separable along the index i. We group the link ij with node i, defining d'^d

$$d'^d(S)_i = \sum_{j:(i,j)\in A} S_{ij} + \sum_{j:(j,i)\in A} \bar{S}_{ji} - 1. \tag{31}$$

Using the preceding definition, we define the following:

$$\begin{aligned}
\bar{\beta}_w &= \{\bar{\beta}_{ij} | i = w\} \\
\bar{\lambda}_w &= \{\bar{\lambda}_{ij} | i = w\} \\
\bar{\mu}_w &= \{\bar{\mu}_i | i = w\} \\
d'^d_w(S) &= \{d'^d(S)_i | i = w\} \\
S_w &= \{S_{ij} | i = w\} \\
d'^s_w(S_w, V) &= \{d'^s_w(S, V)_{ij} | i = w\}.
\end{aligned}$$

The partitioned form of RP-FLAP is the Single Node Relaxed Primal FLAP $(\mathrm{SNRP\text{-}FLAP}_w)$ for each index w

$[\mathrm{SNRP\text{-}FLAP}_w]$

$$\max_{S} \quad \bar{\beta}_w^T S_w + \bar{\lambda}_w^T d'^s_w(S_w, V_w) - \bar{\mu}_w^T d'^d_w(S_w) \tag{32a}$$

$$\text{s.t.} \quad S_{wj} \leq V_w \qquad \forall_j. \tag{32b}$$

The preceding series of decompositions replace the relaxed primal problem (RPP) with $2N$ easy subproblems that can be solved in parallel. Each instance of SNARP_i is a linear program with $|P|$ variables and 1 general constraint. By Proposition 3.2, it can be solved by simply enumerating the objective value for each $p \in P$, of which there are a small constant number, and choosing the pattern with the highest value. Therefore, the overhead of a general-purpose solver can be avoided. Each instance of SNRP-FLAP is a linear problem with $O(N)$ variables and constraints, although it will be further reformulated to avoid oscillation.

D. Economic Interpretation

The dual-problem formulations can be interpreted in the following way: In the coupling between the RMP and CLAP, the dual values $\bar{\beta}_{ij}$ represent the estimated value in terms of improvement to the overall schedule of accommodating more traffic on link ij. In the coupling between Lagrangian subproblems, $\bar{\lambda}_{ij}$ is the *signal quality price*: It represents the value of improving the SINR on link ij, and *duplex price* $\bar{\mu}_i$ represents the value of decreasing the usage of node i.

In SNRP-FLAP, each node activates links to maximize its utility, where $\bar{\beta} \geq 0$ is the reward for activating each link, $\bar{\lambda} \geq 0$ is the penalty for any SINR reduction on each link, and $\bar{\mu} \geq 0$ is the penalty for using each node. In SNARP, each node chooses antenna gains to maximize a different utility, defined solely in terms of $\bar{\lambda}$. This is analogous to the use of *interference price* in

[12] and [13]. When all the constants have their values substituted in, the objective function of SNARP_i is of the form

$$\max_{D_{ij}} \quad \sum_{j \neq i} D_{ij} k_{ij}$$
$$k_{ij} \begin{cases} \geq 0, & \text{if } ij \text{ or } ji \text{ is an active link} \\ \leq 0, & \text{if } ij \text{ or } ji \text{ is an ``interference link''} \\ = 0, & \text{otherwise} \end{cases} \tag{33}$$

where the actual value of constant k_{ij} is determined by $\bar{\lambda}$, node j's antenna configuration, and RF parameters Lb, P, and Nr.

E. Lagrange Multiplier Updates

The combined problems $\mathrm{SNRP\text{-}FLAP}_i$ and SNARP_i for all nodes i implement the relaxed primal problem. Solving proceeds by iteratively solving the RPP and updating the Lagrange multipliers λ and μ so that they converge to an optimal solution of the dual problem. We use a *subgradient* method because it lends itself to distributed implementation and scales well with the problem size. At time t, let s^t denote the degree of constraint violation, α^t denote the step size, and $[\cdot]_+$ denote projection onto the nonnegative orthant. The subscripts λ and μ are used to distinguish the values pertaining to each set of Lagrange multipliers

$$\begin{aligned} s^t_\lambda &= d^s(S^t, D^t, V^t) \\ s^t_\mu &= d^d(S^t) \\ \bar{\lambda}^{t+1} &\leftarrow \left[\bar{\lambda}^t + \alpha^t_\lambda s^t_\lambda\right]_+ \\ \bar{\mu}^{t+1} &\leftarrow \left[\bar{\mu}^t + \alpha^t_\mu s^t_\mu\right]_+ . \end{aligned}$$

We define step size rule $\alpha^t = \frac{a}{(t+b)}, a > 0,\ b \geq 0$. The a and b are tunable parameters and are not related to Guan's a and b in SDQ-FLAP and [33].

1) Convergence Properties: The subgradient method described above will produce optimal values of the Lagrange multipliers for CLAP-dual-2.

Proposition 3.3: The sequences $\{\bar{\lambda}^t\}$ and $\{\bar{\mu}^t\}$ converge to $\lambda^* \in \boldsymbol{\lambda^*}$ and $\mu^* \in \boldsymbol{\mu^*}$, where $(\boldsymbol{\lambda^*}, \boldsymbol{\mu^*})$ are the optimal sets of CLAP-dual-2.

It does not follow that the sequence of *primal* values produced will converge to the desired solution, even when the problems exhibit strong duality. Let S^*, D^* denote solutions to the continuous relaxation of CLAP, and $\hat{S}, \hat{D}$ denote estimates thereof. Define the following sequence:

$$\hat{S}^t = (1 - \alpha^t)\hat{S}^{t-1} + \alpha^t S^t. \tag{34}$$

Proposition 3.4: $\{\hat{S}^t\}$ converges to S^*, and the analogous $\{\hat{D}^t\}$ converges to D^*.

Propositions 3.3 and 3.4 together imply that the subgradient method for multiplier updates correctly solves the Lagrangian dual problem, and that this produces optimal solutions to the primal (CLAP) problem, subject to the following caveat: There is a limitation to Proposition 3.4, which was not made clear in [30]. Recall that we relax the 0–1 constraints from JBSS-MP and CLAP—which are unavoidably nonconvex—and rely on the integrality properties of the decomposed relaxed primal problems to produce feasible results. This implies that while the RPP at every subgradient iteration will have integer values, the solution may oscillate between integer points, leading to a noninteger mean. Though we have not observed this in practice, neither have we proved that it cannot occur. A rounding algorithm is given in Section III-G to address this possibility.

Our formulation exhibits a well-known issue with subgradient methods: Small changes in the Lagrange multipliers produce large changes in primal solutions, causing oscillation around the ideal search trajectory. This can slow the solution process. The linear objective function and previously mentioned integrality property contribute to this behavior in FLAP and its derived problems. Additionally, when the relevant SINR prices λ are 0 and the $\bar{\beta}$ values are the same, links that share a node exhibit the *homogeneous subproblem* property where any given dual price μ will result in the same primal outcome for all links. This issue arises in the context of the hydrothermal *unit commitment* problem and is commonly addressed using surrogate subgradient methods. To simplify decentralized implementation, however, we instead use a nonlinear approximation method of the form presented in [33]. This is conceptually very similar to an augmented Lagrangian, but the additional quadratic parameter is computed locally for each subproblem, maintaining the separable structure of the original program. Based on this transformation, we introduce the Single-node Dual Quadratic FLAP, or SDQ-FLAP. SDQ-FLAP maximizes a quadratic approximation ${a_{ij}S_{ij}}^2 + (b_{ij} - \bar{\lambda}_{ij}S_{ij}) \approx \beta_{ij}S_{ij} + \bar{\lambda}_{ij}{d'}^s(S_{ij})$, where a_{ij} and b_{ij} are constants updated at each iteration [33]. Exact definitions are given in [3, Listing D.4]

$[\mathrm{SDQ\text{-}FLAP}_i]$

$$\max_{S} \quad \sum_{j:ij \in A} -{a_{ij}S_{ij}}^2 + (b_{ij} - \bar{\lambda}_{ij}S_{ij}) - \frac{\bar{\mu}_i + \bar{\mu}_j}{2} S_{ij} \tag{35a}$$

$$\text{s.t.} \qquad S_{ij} \leq V_i \qquad \forall_j. \tag{35b}$$

Proposition 3.5: Any stable solution to $\mathrm{SDQ\text{-}FLAP}_i$ is also a solution to $\mathrm{SNRP\text{-}FLAP}_i$.

The preceding formulation significantly reduces oscillation relative to FLAP or its decomposed analog, SNRP-FLAP. The constraint (35b) can be ignored: The variable V_i does not appear in the objective function and is otherwise free, so the problem can be solved for S and V_i chosen to be $\max(S_{ij})$. $\mathrm{SDQ\text{-}FLAP}_i$ is therefore an *unconstrained* (or bound-constrained) quadratic program with at most $N + 1$ variables. For any reasonable N, this is easy to solve.

F. Partial Pricing

Recall that the objective of the column generation subproblem is to find improving feasible points for inclusion in the restricted master problem. The optimality of the overall result does not require that the subproblem finds the *most* improving point, only that it finds *an* improving point if one exists. We exploit this by using "partial pricing" and returning the first improving primal feasible result $(\hat{S}^t, \hat{D}^t)$—which may or may not be the best possible—without waiting for the subgradient process to converge [34]. It is only necessary to allow the subproblem to fully converge to prove that there

is no as-yet-undiscovered feasible improving point. Heuristic rounding is performed in this step to extract an integer solution from an estimate $\hat{S}$ that is not yet converged. We round by finding the least level thr for which $(S^{\text{int}}, \hat{D})$, defined as follows:

$$S_{ij}^{\text{int}} = \begin{cases} 1, & \hat{S}_{ij} \geq thr \\ 0, & \hat{S}_{ij} < thr \end{cases}$$

is a feasible solution. This value of thr is found by simple binary search in a constant (and small) number of steps.

Every solution to an iteration of the restricted master problem is a valid schedule. Each such schedule can be put into place in the network immediately if it is superior to the current schedule, regardless of whether or not it is the final, best schedule. Consequently, terminating the subproblem early and resolving the RMP yields a possibly useful result sooner than solving the subproblem to optimality, even though it may or may not improve the overall running time.

G. Amenability to Randomized Rounding

In every experimental scenario considered (see Section IV), we observe that $\hat{S}$ and $\hat{B}$ converge to integer solutions, and therefore the heuristic rounding described above is merely a running-time optimization. This problem is also amenable to a randomized rounding solution, which covers the possibility of a fractional solution with a provable (but loose) approximation-and-integrality ratio. One approach is as follows: First, the constraint matrix is sparsified in a way that maintains feasibility at the cost of a finite reduction in utility. This reduces the constraint-constraint dependency such that, with further scaling, the Lovász Local Lemma (LLL) demonstrates the existence of a satisfying assignment [35].

1) Sparsification: Given an optimal fractional solution $(S*, B*)$ with value OPT, the problem is first simplified in two ways. Variable fixing removes (rounds to 0) the lowest-utility links: Given parameter $\delta_1 \in [0,1]$ choose any set of links $I \subseteq 2^A$ s.t. $\Sigma_{ij \in I} \bar{\beta}_{ij} S^*_{ij} \leq \delta_1 \bar{\beta}^T S^*$. A maximal I can be found greedily. By definition, removing I reduces the utility by δ_1. For each link ij, column-sparsification removes (sets to 0) the SINR constraint coefficients for δ_2-*irrelevant* links: Given any $\delta_2 \in [0,1]$, choose any $S_{ij} \subseteq 2^A$ s.t. $\Sigma_{k:kl \in S_{ij}} \text{rx\_power}(k,j) \leq \delta_2 \text{ interference\_margin}(ij)$. Scaling S to $(1-\delta_2)S^*$ maintains feasibility while reducing utility by δ_2. These reduce the maximum degree of the constraint hypergraph from $|A| = O(|N|^2)$ to a density-dependent constant and reduce the utility to $(1-\delta_1)(1-\delta_2)OPT$.

2) Approximation: Replacing each S_{ij} with random variable X_{ij} on $\{0,1\}$ with $\Pr[X_{ij}=1] = \gamma(1-\delta_2)S^*_{ij}$ we can then apply the following "generic" algorithm: We derive Chernoff–Hoeffding bounds on the probability that any given constraint is violated (as a function of γ). The column-sparseness property gives a constraint-constraint dependency degree bound d s.t. for a properly chosen γ, a satisfying assignment exists by the LLL. Finally, Moser and Tardos' algorithm [36] gives such an assignment in $O(|A|^2)$ time. Following [37, Theorem II.2], this assignment comes from the *conditional LLL distribution* that approximates the original distribution on X within $\eta = \Pi_{C \in \Gamma_{\mathcal{A}}(B)}(1-X_C)^{-1}$. This gives an expected utility of $(1-\delta_1)(1-\delta_2)(\frac{1}{\gamma})(\frac{1}{\eta})OPT$. This gives an $O(1)$ bound, but the constants are not tight—e.g., choosing $\delta_1, \delta_2, \gamma$, and η for the worst observed data gives an approximation factor of ≈ 2 relative to the fractional solution.

Algorithm 1: CHECK-MASTER

repeat
  $\hat{S}, \hat{D} \leftarrow$ `BLOCKING_RECV()`
  $S', D \leftarrow$ `PARTIAL_PRICE`$(\hat{S}, \hat{D})$
  if (S', D) *feasible and new* **then**
    $L_A \leftarrow L_A \cup S'$
    $x, \beta \leftarrow$ `RMP`(L_A)
    `BROADCAST`(β)
    if x *better than previous* **than**
    `BROADCAST`(x)
until *forever*

H. Distributed Consensus

The preceding sections decompose the original JBSS problem into a form where $2N$ small problems are solved in parallel for each subgradient update iteration. Going from a parallel algorithm to a distributed one requires some consideration of the communication processes. We make use of a very simple and robust model due to [38] and [39]: Every node maintains its own version of every variable, and nodes announce their variable values to other nodes occasionally. This occurs concurrently with the subgradient algorithm: Each node locally computes values for its designated subproblems and the Lagrange multipliers and passively tracks its neighbors' values for other variables. Upon computing a new value or receiving other nodes' variable values, a node updates its own values according to a weighted averaging scheme. Under light requirements on the weights and communication frequencies, it is shown that this scheme has the same convergence properties as its centralized counterpart. This means that our distributed, asynchronous algorithm has the same *correctness* as a centralized one.

I. Summary

These decompositions produce a distributed algorithm that is equivalent to the JBSS-MP up to a potential duality gap between CLAP and CLAP-dual-1 (24). The distributed algorithm resulting from these decompositions consists of two asynchronous parts: one or more processes running the rounding, partial pricing and RMP computations, and one process per node running an instance of the dual subproblems. The subproblems are asynchronously, and the step sizes and message-broadcasting rules are tuned to make SNARP operate on a faster timescale as in [40, Sec. V]. These processes are coarsely sketched in Algorithms 1 and 2, respectively. Empirical performance results are given in Sections IV and V.

IV. Numerical Experiments

Though Section III showed a series of decompositions intended to allow the original problem to be solved efficiently, it

Algorithm 2: DUAL-SUBPROBLEMS$_i$

repeat
  /* For node$i$: Define $S_{[i]}=S_{j:ij\in A}$, $D_{[i]}=D_{ik}\ \forall k$, $B_{[i]}=B_{ip}\ \forall p$ */
  remote vars $\leftarrow$ BLOCKING_RECV()
  if *new* β**then**
    RESET
  $\hat{S},\hat{D},\hat{B} \leftarrow$ CONSENSUS_UPDATE (remote vars)
  if CHANGED$(\hat{S},\hat{D},\hat{B})$ **then**
    $S_{[i]} \leftarrow$SDQ $-$ FLAP$_i(\hat{S},\hat{D},\hat{B})$
    $D_{[i]},B_{[i]} \leftarrow$SNARP$_i(\hat{S},\hat{D},\hat{B})$
    $\bar{\mu},\bar{\lambda} \leftarrow$ SUBGRADIENT_STEP$(\hat{S},\hat{D},\hat{B})$
    $\hat{S},\hat{D},\hat{B} \leftarrow$ CONSENSUS_UPDATE $(S_{[i]},D_{[i]},B_{[i]},\bar{\mu},\bar{\lambda})$
    foreach v *in* $\hat{S},\hat{D},\hat{B}$ **do**
      if CHANGED(v) **then**
        BROADCAST(v)
      else
        maybe BROADCAST(v)
until *termination*

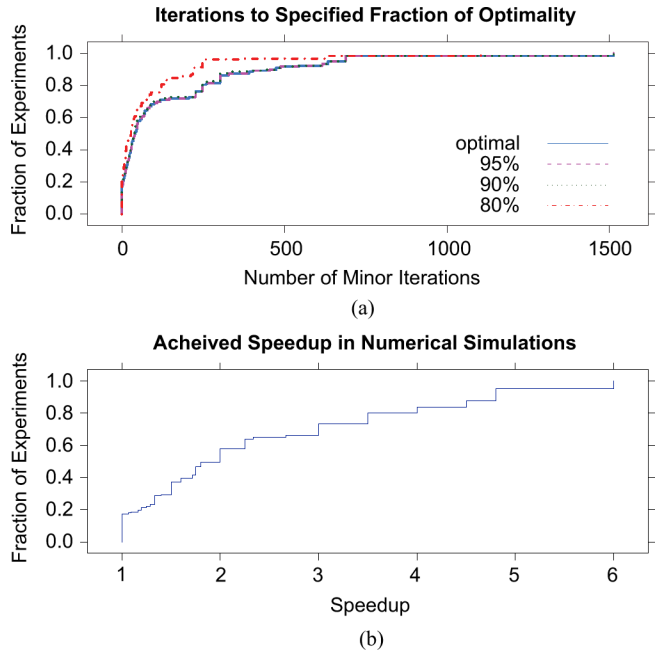

Fig. 5. Performance in simulations. (a) ECDF of minor iterations required to reach optimal solution, or specified fraction of optimality, in simulation. (b) Empirical cumulative distribution of achieved speedup (ratio of optimal to TDMA performance) across all simulations.

remains in principle NP-hard. This section presents numerical results showing that, despite an exponential theoretical worst case, the running time and scaling properties observed in practice are very good. These experiments emulate a distributed algorithm in that each node's computations are performed separately. Experiments were conducted by running the algorithm over a large number of scenarios constructed with varying initial values. In total, 1396 experiments were run. The following major parameters were varied: number of nodes (between 0 and 48), number of links (between $\frac{1}{2}$ and 3 per node), and size of the simulated region (between 1 and 16 square km). For each set of parameters, nodes were randomly placed within the simulated area with uniform probabilities, and pairwise path losses were estimated using the Green–Obaidat model [41]. All possible links were identified based on a hypothetical transmission power of 14.7 dBm, a required signal strength of -80 dBm, and the best-case antenna gains given a measured phased-array antenna beam pattern. The requested number of links were chosen randomly from the pool of possible links; if enough possible links did not exist then a new layout was generated. The results presented here are aggregates across all of these scenarios—a full factorial analysis is planned for future empirical studies of these algorithms and associated STDMA MAC.

A. Running Time

A well-known limitation of subgradient methods for updating Lagrange multipliers is that they are very slow to reach a provably converged state. This means in practice that such algorithms may find optimal values relatively quickly, but then require a longer period to verify that no better values exist. As alluded to in Section III-F, *termination* may not be the best criterion for an online system. It is expected that schedule optimization will be a continuous process, converging and diverging as system parameters change. Consequently, we find it useful to examine the time required to find optimal and near-optimal solutions as well as the time to termination.

To quantify the behavior, see Fig. 5(a), which plots the distribution of the number of iterations required to first reach the optimal solution across all of our simulation runs. Although some scenarios may require as many as 1500 iterations to settle on the optimal solution, we can see that in more than 90% of the cases, the optimal solution is found within 500 iterations (the mean is 150 iterations and 91.83% are solved to optimality within 500). On average, we are able to get within 10% of optimal within 146 iterations and within 20% of optimal within only 85 iterations.

In our experiments, we find that execution time (whether measured by time to optimality or time to termination) is *at worst* linear in the size of the input. Fig. 6 shows the iterations required to find an optimal solution over all the input cases.

B. Schedule Efficiency

In addition to convergence properties, our numerical experiments provide a window into the ability of the algorithm to produce efficient (high-reuse) schedules across a large number of randomly generated scenarios. Fig. 5(b) plots a speedup metric that is the ratio of the time required by a TDMA MAC to service a given demand relative to the time required by our optimized system. This is either an increase in throughput, given a fixed amount of time, or an increase in free spectrum time, given a fixed workload. In our experiments, we see speedup values ranging from 1 (no speedup) to 6 with an average speedup of 2.34 across all scenarios ($\sigma = 1.31$).

In an empirical comparison to a direct global solution, we find a zero duality gap in 75% of cases. For those cases with a nonzero duality gap, the mean speedup is 71% of that found

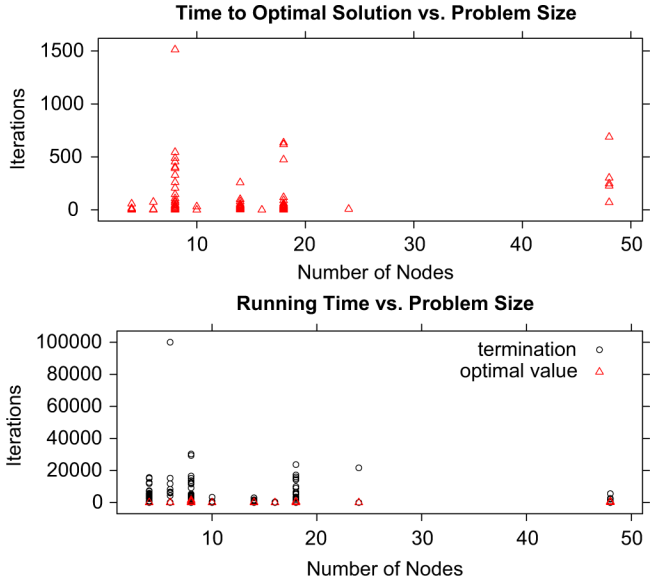

Fig. 6. Execution time relative to problem size. Note that the y-axis scale differs on the two subplots. By either measure, the complexity is no worse than linear over this domain.

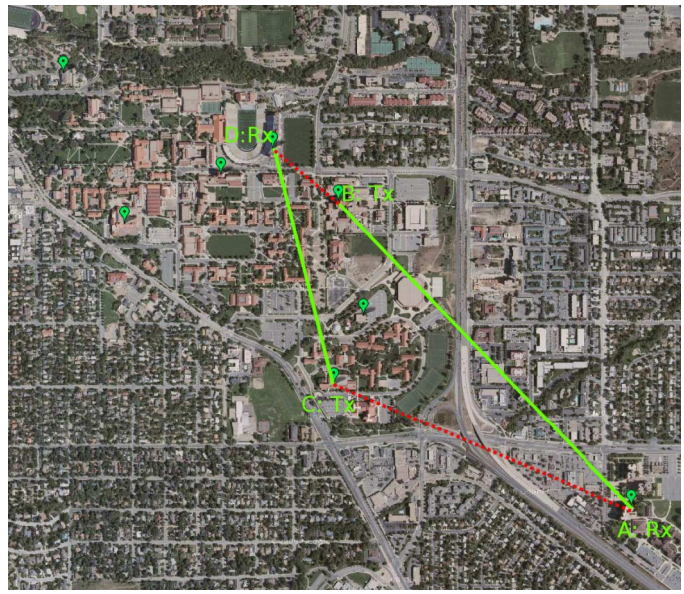

Fig. 7. Outdoor testbed: links B → A and C → D shown.

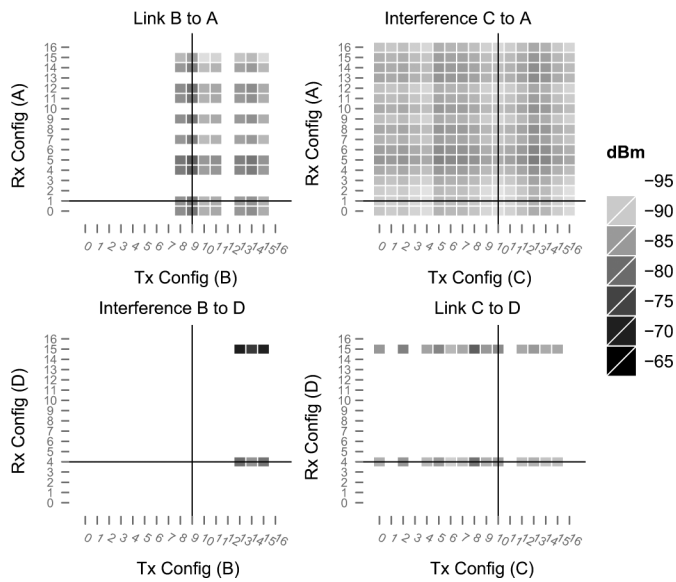

Fig. 8. Antenna configuration effects on all four links (signal or interference). Undetectable signals are classified as −95 dBm.

by the global solution. This comparison was performed only for relatively small instances (up to 24 nodes) because the execution time for the global solver became prohibitive.

V. Deployed System

Thus far, this paper has described and evaluated our *mathematical* design; this section addresses its concrete implementation. The system we present here operates in a *fully distributed*, *asynchronous* manner. Nodes maintain and exchange variables as described in Section III-H.

In addition to the subproblem solver processes, there is a separate process for the rounding, partial pricing, and RMP. When this process detects that its current estimates $(\hat{S}^t, \hat{D}^t$ constitute a primal feasible solution with negative reduced cost, a corresponding new column is added to the RMP. The RMP is resolved to make use of this information, and the resulting new schedule, updated dual prices $\bar{\beta}$, and step-size reference time are sent to all nodes by a flooding protocol. The new schedule is put into effect immediately, and computation continues. The implementation is described in more detail in [3, Sec. 6.3.1].

A. Test Scenario

This system was deployed on the CU-WART wide-area phased-array antenna testbed [1], shown in Fig. 7. When these experiments were run, the testbed had six operational nodes, allowing at most three concurrent links. With this particular hardware and layout, there are no feasible three-link combinations, but several two-link combinations are possible. The remainder of this section walks through the scheduling and configuration process for one of these two-link combinations.

For this experiment, we offered a constant bit-rate (CBR) stream of UDP packets with 1024-B payloads on links B → A and C → D. For clarity, we have chosen an example in which the best schedule (only those links active) is obvious. However, it is important to note that: 1) the scheduler was not preconfigured to know that this schedule was possible; and 2) the same configuration and combination of links is successfully identified in larger experiments.

This pair of links forms an interesting example because it *requires* a nonobvious physical-layer configuration on *both* links to be feasible. With naive beam-steering, these links are bad neighbors—node C will cause substantial interference at node A (62.5 dBm on average). In fact, if *either* link chooses its local best configuration, there is *no* possible configuration of the other link that makes the combination feasible! This means that neither a configure-then-schedule approach nor a greedy add-and-configure-links approach like [25] and [26] will identify this as a possible combination.

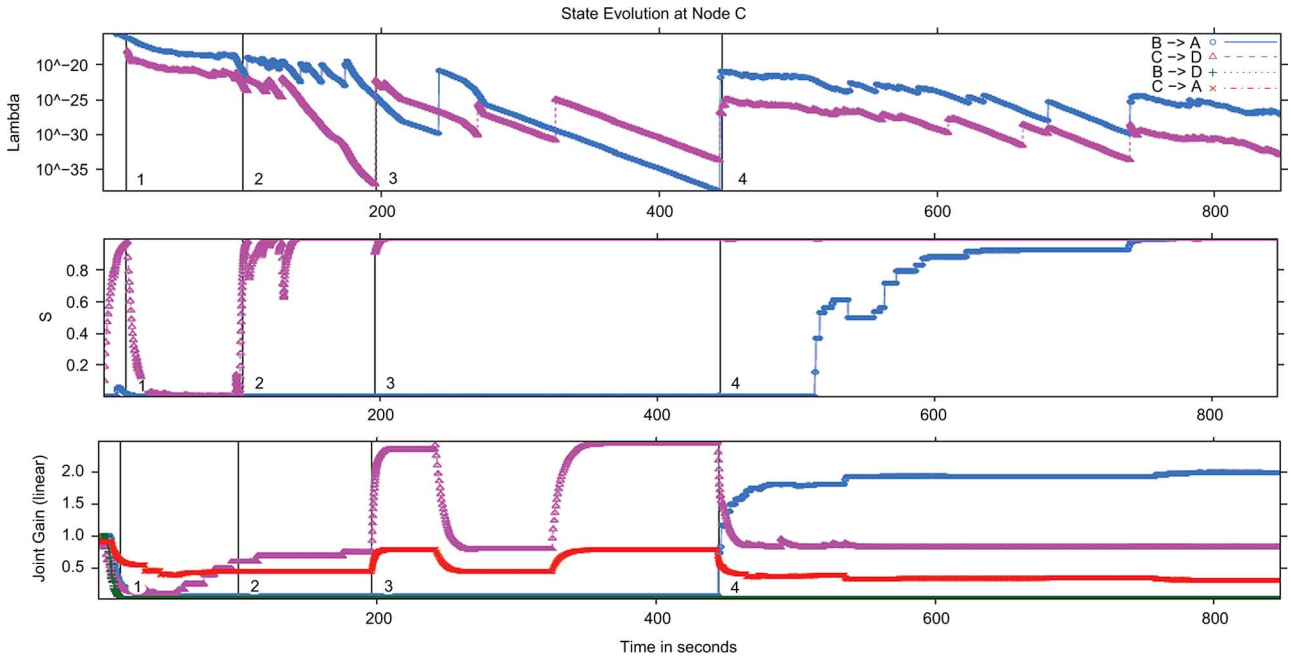

Fig. 9. Trace of algorithm scheduling links B → A and C → D concurrently, as seen locally at node C. The top strip shows $\bar{\lambda}$, middle strip shows $\hat{S}$, and the bottom strip shows the *combined* gain $\hat{D}_{ij}\hat{D}_{ji}$. Note that B → D and C → A are interference if both data links are active. The aligned x-axis is time in seconds.

B. Outcome

Fig. 8 shows the configuration to which our algorithm converges: The heat maps show the signal (or interference) strength between the nodes for all combinations of antenna configuration, and the cross-hairs indicate the configuration chosen. In both the "Link B to A" (upper left) and "Link C to D" (lower right) heat maps, the configuration chosen is 5–10 dBm worse (lighter) than the best available. Intuitively, one can see that the *interference* from C to A is the dominating constraint: Most configurations of C and A would make that interference stronger than the intended signal.

C. Execution Process

Fig. 9 shows the execution of the algorithm in the scenario described above, as observed by a single node (C). The top strip of this figure shows the evolution of the SINR Lagrange multiplier estimates $\bar{\lambda}$, the *signal quality prices*, the second strip shows the consensus estimated link activations $\hat{S}$, and the third strip shows the combined antenna gains for the signals and interference. Times of interest are marked with a vertical bar and labeled $(1, 2, \ldots)$ on all strips. No change to actual system state occurs until a new execution of the RMP: The link activation and antenna configurations referred to are variable values. Qualitatively, the execution of the algorithm can be understood in the following stages.

Prior to time 1, node C's estimate $\bar{\lambda}_{\mathrm{CD}}$ is 0. This drives the link activation $\hat{S}_{\mathrm{CD}}$ toward 1, while the SNARP objective is undefined and the resulting gains are low.

At time 1, high activation and low gain causes the SINR constraint for link C → D to be violated. The price $\bar{\lambda}_{\mathrm{CD}}$ takes a large step to $> 10^{-20}$. This drives $\hat{S}_{\mathrm{CD}}$ back toward 0 and causes $\hat{D}_{\mathrm{CD}}\hat{D}_{\mathrm{DC}}$ to start increasing. The price $\bar{\lambda}_{\mathrm{CD}}$ decreases as the low activation and higher gain stay within the constraints.

At time 2, the combination of low $\bar{\lambda}_{\mathrm{CD}}$ and higher gain allows $\hat{S}_{\mathrm{CD}}$ to increase to near 1. At time 3, $\hat{S}_{\mathrm{CD}}$ gets close enough to 1 to violate the SINR constraint again and drive up $\bar{\lambda}_{\mathrm{CD}}$. The increase in $\bar{\lambda}_{\mathrm{CD}}$ relative to $\bar{\lambda}_{\mathrm{BA}}$ drives the antennas to favor $\hat{D}_{\mathrm{CD}}\hat{D}_{\mathrm{DC}}$. Note that this antenna configuration at node C has high gain toward A, raising the unwanted gain $\hat{D}_{\mathrm{CA}}\hat{D}_{\mathrm{AC}}$.

Between times 3 and 4, $\bar{\lambda}_{\mathrm{CD}}$ and $\bar{\lambda}_{\mathrm{BA}}$ trend down, but changes in their relative magnitude cause the antenna state to switch back and forth. Immediately before time 4, $\hat{S}_{\mathrm{BA}}$ increases almost invisibly. Recall that node C is *not computing* S_{BA}, so a change in $\hat{S}_{\mathrm{BA}}$ reflects the incorporation of a value broadcast by node B. This change is sufficient to cause an SINR constraint violation, driving $\bar{\lambda}_{\mathrm{BA}}$ up at time 4.

Note two changes with regard to the gains: First $\hat{D}_{\mathrm{AB}}\hat{D}_{\mathrm{BA}}$ increases dramatically, reflecting a change in antenna configuration by node B. Second, the change in $\bar{\lambda}_{\mathrm{BA}}$ causes node C to change its antenna configuration to diminish $\bar{D}_{\mathrm{CA}}$, at the cost of also reducing $\bar{D}_{\mathrm{CD}}$. This new configuration can accommodate both links, and $\hat{S}_{\mathrm{BA}}$ tends toward 1 as node C receives updates from other nodes. At this point, the RMP can schedule the two links concurrently with the configuration given. Note that $\bar{\lambda}$ continues to vary but this variation does not affect the primal estimates.

The prototype implementation used in these experiments contains significant inefficiencies, described in more detail in [3] and [30]. A clean reimplementation of the same algorithms reduces the computation time by a factor of 10^5. We expect that the communication process can similarly be improved, though not by as dramatic a factor.

VI. Conclusion

This paper presents a price-coupled decomposition structure for jointly optimizing *which users* communicate *when* and *how*. Using this structure, we solve the joint beam steering and

scheduling problem. Optimal spatial reuse TDMA scheduling is known to be NP-hard, and the addition of antenna configuration increases the state space *exponentially* in the number of nodes. In solving this problem, we provide the *first implementation of wireless scheduling based on dual decomposition of signal constraints*. These algorithms are computationally efficient—they find solutions within hundreds of iterations, each of which requires only minimal computation. Despite the NP-hard nature of the underlying problem, our running time appears linear in the problem size in practice. The algorithm makes very few assumptions about the patterns of the antennas' directionality or the environment's path loss.

While there is some complexity in the decomposition process, the resulting system is very simple: Using shared measurements and prices, nodes make local utility-maximizing choices about whether or not to be active, and if so, with what configuration. These choices are exchanged, used to update prices, and acted on if they do not create a conflict. With slight variations, this "template" can be realized as a real-time online MAC, adapted to multiple physical-layer "knobs," and integrated with a variety of higher-layer utility models.

Though subject to some convexity requirements, the pattern of *signal quality price decomposition* generalizes to a wide range of joint optimization problems involving interacting radio-frequency systems [3]. We firmly believe that optimization decomposition is a paradigm that will drive next-generation wireless networks, and we offer our work here as an important step toward realizing the theoretical gains of this approach in real systems.

APPENDIX
PROOFS OF DECOMPOSITION PROPERTIES

Proof of Proposition 3.1: The constraint matrix of continuous FLAP is totally unimodular by Ghouila–Houri's Theorem. Therefore, every extreme point of the feasible polytope is in $\mathbb{Z}^n$. The objective is concave, implying that no maximum occurs within the feasible polytope, and thus that the constrained optimum occurs at an extreme point. Therefore, the integer and continuous optima occur at the same point. The inverse of the constraint matrix is also totally unimodular by Cramer's Rule, and so the same holds for the dual. ■

Proof of Proposition 3.2: SNARP_i is a linear program in D, B, but can be rewritten purely in B by substituting $\Sigma_{p\in P} G_{ikp} B_{ip}$ for D_{ik} in the objective function. So written, it is a linear program with $|P|$ variables and $2|P|+1$ constraints. By the fundamental theorem of linear programming [42, Theorem 3.4], there exists a basic solution in which $|P|$ constraints are satisfied with equality. Constraint (26c) must be one of them. This forces $|P|-1$ out of (26d), (26e) to be satisfied with equality, which means that $|P|-1$ of the variables must be either 0 or 1. Those variables must then sum to either 0 or 1, based on (26c). Those options force the remaining variable to be 1 or 0, respectively, in order to satisfy (26c). ■

Proof of Proposition 3.3: Let X be the set of all decision variables, x be a vector value in X, and x_0 be some specific value of x, *not* a scalar component of x. Let G_s be any subgradient of d'^s and G_d be any subgradient of d'^d. Then, $\lambda G_s(x_0) + \mu G_d(x_0)$ is a subgradient of $-\bar{\beta}^T S + \lambda^T d^s(S,D,V) + \mu^T d^d(S)$, by Shor's [43, Theorem 15]. This equals (28). Therefore, $S^t_\lambda + S^t_\mu$ is a subgradient of (28). The sum over all i of t SNRP-FLAP_i and SNARP_i equals the objectives and constraints of CLAP-dual-2. Assume that the Slater condition holds, otherwise the problem and JBSS-MP are infeasible. The series $\Sigma_{t=0}^{\infty} \frac{a}{(t+b)^n}$ $0 < n \leq 1$ diverges and $\lim_{t\to\infty} \alpha^t = 0$ for $n, a > 0$. Therefore, $\{x\}$ converges to x^* by [43, Theorem 31]. ■

Proof of Proposition 3.4: We appeal to a result by Larsson *et al.* [44]. $\{\hat{S}^t\}$ is generated by a subgradient process satisfying criteria (9)–(11). $\{\hat{S}^t\}$ is an ergodic sequence satisfying (7) and (13). It follows from [44, Theorem 1] that $\{\hat{S}^t\}$ converges to the solution set. The same applies to $\{\hat{D}^t\}$. ■

Proof of Proposition 3.5: The constraints of SDQ-FLAP_i are identical to those of FLAP_i. At any point x_0, the nonlinear approximation f' generated at x_0 is parallel to f[33]. For both SDQ-FLAP and SNRP-FLAP, the constraints are all differentiable and convex, and the objective is convex (when stated as minimization). Therefore, the Karush–Kuhn–Tucker (KKT) conditions are sufficient for global optimality.

Let x^* be an optimal solution of SDQ-FLAP_i as constructed at x_0. The KKT conditions therefore hold. Assume x^* is stable, therefore $x^* = x_0$. Suppose that x_0 is not an optimal solution of SNRP-FLAP_i. The KKT conditions other than stationarity are the same in both cases, so they must hold for SNRP-FLAP_i. Therefore, the stationarity condition must hold for SDQ-FLAP_i but not for SNRP-FLAP_i. That requires, for the same constraints, that $\nabla f'(x^*) \neq \nabla f(x^*)$, $\perp$. ■

REFERENCES

[1] E. Anderson, C. Philips, G. Yee, D. Sicker, and D. Grunwald, "Challenges in deploying steerable wireless testbeds," in *Proc. TridentCom*, 2010, pp. 231–240.

[2] R. L. Freeman, *Radio System Design for Telecommunications*, 2nd ed. New York, NY, USA: Wiley-Interscience, 1997.

[3] E. W. Anderson, "Integrated scheduling and beam steering for spatial reuse" Ph.D. dissertation, Dept. Comput. Sci., University of Colorado, Boulder, CO, USA, 2010 [Online]. Available: http://www.ece.cmu.edu/~andersoe/

[4] E. Arikan, "Some complexity results about packet radio networks," *IEEE Trans. Inf. Theory.*, vol. IT-30, no. 4, pp. 681–685, Jul. 1984.

[5] S. Toumpis and A. J. Goldsmith, "Capacity regions for wireless ad hoc networks," *IEEE Trans. Wireless Commun.*, vol. 2, no. 4, pp. 736–748, Jul 2003.

[6] F. P. Kelly, A. K. Maulloo, and D. K. H. Tan, "Rate control for communication networks: Shadow prices, proportional fairness and stability," *J. Oper. Res. Soc.*, vol. 49, no. 3, pp. 237–252, 1998.

[7] P. Björklund, P. Varbrand, and D. Yuan, "Resource optimization of spatial TDMA in ad hoc radio networks: A column generation approach," in *Proc. IEEE INFOCOM*, 2003, vol. 2, pp. 818–824.

[8] L. Xiao, M. Johansson, and S. Boyd, "Simultaneous routing and resource allocation via dual decomposition," *IEEE Trans. Commun.*, vol. 52, no. 7, pp. 1136–1144, Jul. 2004.

[9] M. Chiang, "Balancing transport and physical layers in wireless multihop networks: jointly optimal congestion control and power control," *IEEE J. Sel. Areas Commun.*, vol. 23, no. 1, pp. 104–116, Jan. 2005.

[10] M. Chiang, *Geometric Programming for Communication Systems*. Hannover, MA, USA: Now, 2005.

[11] M. Chiang, S. Low, A. Calderbank, and J. Doyle, "Layering as optimization decomposition: A mathematical theory of network architectures," *Proc. IEEE*, vol. 95, no. 1, pp. 255–312, Jan. 2007.

[12] C. W. Tan, D. Palomar, and M. Chiang, "Exploiting hidden convexity for flexible and robust resource allocation in cellular networks," in *Proc. IEEE INFOCOM*, 2007, pp. 964–972.

[13] C. W. Tan, D. Palomar, and M. Chiang, "Energy-robustness tradeoff in cellular network power control," *IEEE/ACM Trans. Netw.*, vol. 17, no. 3, pp. 912–925, Jun. 2009.
[14] C. W. Tan, M. Chiang, and R. Srikant, "Fast algorithms and performance bounds for sum rate maximization in wireless networks," in *Proc. IEEE INFOCOM*, 2009, pp. 1350–1358.
[15] A. Eryilmaz, O. Asuman, and E. Modiano, "Polynomial complexity algorithms for full utilization of multi-hop wireless networks," in *Proc. IEEE INFOCOM*, 2007, pp. 499–507.
[16] A. Gupta, X. Lin, and R. Srikant, "Low-complexity distributed scheduling algorithms for wireless networks," *IEEE/ACM Trans. Netw.*, vol. 17, no. 6, pp. 1846–1859, Dec. 2009.
[17] C. W. Tan, S. Friedland, and S. H. Low, "Spectrum management in multiuser cognitive wireless networks: Optimality and algorithm," *IEEE J. Sel. Areas Commun.*, vol. 29, no. 2, pp. 421–430, Feb. 2011.
[18] J. B. Cain, T. Billhartz, L. Foore, E. Althouse, and J. Schlorff, "A link scheduling and ad hoc networking approach using directional antennas," in *Proc. IEEE MILCOM*, 2003, vol. 1, pp. 643–648.
[19] L. Bao and J. J. Garcia-Luna-Aceves, "Transmission scheduling in ad hoc networks with directional antennas," in *Proc. ACM MobiCom*, 2002, pp. 48–58.
[20] A. Deopura and A. Ganz, "Provisioning link layer proportional service differentiation in wireless networks with smart antennas," *Wireless Netw.*, vol. 13, no. 3, pp. 371–378, 2007.
[21] K. Sundaresan, W. Wang, and S. Eidenbenz, "Algorithmic aspects of communication in ad-hoc networks with smart antennas," in *Proc. ACM MobiHoc*, 2006, pp. 298–309.
[22] W.-D Wirth, *Radar Techniques Using Array Antennas*. London, U.K.: IET, 2001.
[23] M. Sánchez and J. Zander, "Adaptive antennas in spatial TDMA multihop packet radio networks," in *Proc. RVK*, 1999.
[24] K. Dyberg, F. Farman, L. Eklof, J. Grönkvist, U. Sterner, and J. Rantakokko, "On the performance of antenna arrays in spatial reuse TDMA ad hoc networks," in *Proc. MILCOM*, 2002, vol. 1, pp. 270–275.
[25] X. Liu, A. Sheth, M. Kaminski, K. Papagiannaki, S. Seshan, and P. Steenkiste, "DIRC: Increasing indoor wireless capacity using directional antennas," in *Proc. ACM SIGCOMM*, 2009, pp. 171–182.
[26] X. Liu, A. Sheth, K. Papagiannaki, S. Seshan, and P. Steenkiste, "Pushing the envelope of indoor wireless spatial reuse using directional access points and clients," in *Proc. MobiCom*, 2010, pp. 209–220.
[27] E. Jorswieck, P. Svedman, and B. Ottersten, "On the performance of TDMA and SDMA based opportunistic beamforming," *IEEE Trans. Wireless Commun.*, vol. 7, no. 11, pp. 4058–4063, Nov. 2007.
[28] P. Björklund, "Applications of resource optimization in wireless networks," Ph.D. dissertation, Linköping Universitet, Linköping, Sweden, 2006.
[29] E. Anderson, C. Phillips, D. Sicker, and D. Grunwald, "Modeling environmental effects on directionality in wireless networks," *Math. Comput. Model.*, vol. 53, pp. 2078–2092, 2011.
[30] E. Anderson, C. Philips, D. Sicker, and D. Grunwald, "Signal quality pricing: Decomposition for spectrum scheduling and system configuration," in *Proc. IEEE DySPAN*, May 2011, pp. 408–419.
[31] L. Chen, S. H. Low, and J. C. Doyle, "Joint congestion control and media access control design for ad hoc wireless networks," in *Proc. IEEE INFOCOM*, 2005, vol. 3, pp. 2212–2222.
[32] M. Johansson and L. Xiao, "Cross-layer optimization of wireless networks using nonlinear column generation," *IEEE Trans. Wireless Commun.*, vol. 5, no. 2, pp. 435–445, Feb. 2006.
[33] X. Guan, P. B. Luh, and L. Zhang, "Nonlinear approximation method in Lagrangian relaxation-based algorithms for hydrothermal scheduling," *IEEE Trans. Power. Syst.*, vol. 10, no. 2, pp. 772–778, May 1995.
[34] J. Desrosiers and M. E. Lübbecke, "A primer in column generation," in *Column Generation*, ser. Groupe d'études et de Recheche en Analyse des Décisions (GERAD) 25th Anniversary, G. Desaulniers, J. Desrosiers, and M. M. Solomon, Eds. New York, NY, USA: Springer, 2005, pp. 1–33.
[35] P. Erdös and L. Lovász, "Problems and results on 3-chromatic hypergraphs and some related questions," *Infinite Finite Sets*, vol. 10, pp. 609–627, 1975.
[36] R. A. Moser and G. Tardos, "A constructive proof of the general Lovász local lemma," *J. ACM*, vol. 57, no. 2, pp. 11:1–11:15, Feb. 2010.
[37] B. Haeupler, B. Saha, and A. Srinivasan, "New constructive aspects of the Lovász local lemma," in *Proc. 51st Annu. IEEE FOCS*, 2010, pp. 397–405.
[38] J. N. Tsitsiklis, D. P. Bertsekas, and M. Athans, "Distributed asynchronous deterministic and stochastic gradient optimization algorithms," *IEEE Trans. Autom. Control*, vol. AC-31, no. 9, pp. 803–812, Sep. 1986.
[39] A. Nedic, D. Berteskas, and V. Borkar, "Distributed asynchronous incremental subgradient methods," in *Inherently Parallel Algorithms in Feasibility and Optimization and Their Applications*. Amsterdam: Elsevier, 2001.
[40] J. Zhang, D. Zheng, and M. Chiang, "The impact of stochastic noisy feedback on distributed network utility maximization," *IEEE Trans. Inf. Theory*, vol. 54, no. 2, pp. 645–665, Feb. 2008.
[41] D. Green and A. Obaidat, "An accurate line of sight propagation performance model for ad-hoc 802.11 wireless LAN (WLAN) devices," in *Proc. IEEE ICC*, 2002, vol. 5, pp. 3424–3428.
[42] V. Chvátal, *Linear Programming*. San Francisco, CA, USA: Freeman, 1980.
[43] N. Z. Shor, *Nondifferentiable Optimization and Polynomial Problems, ser. Nonconvex Optimization and its Applications*. Norwell, MA, USA: Kluwer, 1998.
[44] T. Larsson, M. Patriksson, and A.-B. Strömberg, "Ergodic, primal convergence in dual subgradient schemes for convex programming," *Math. Program.*, vol. 86, pp. 283–312, 1999.

Eric Anderson (M'11) is a System Scientist with the Department of Computer Science, Carnegie Mellon University, Pittsburgh, PA, USA. He was previously a Postdoctoral Fellow with the Department of Electrical and Computer Engineering, Carnegie Mellon University. His research interests include networking, wireless communication, and algorithms.

Caleb Phillips (A'12) is an Assistant Professor Adjunct with the University of Colorado, Boulder, CO, USA. He has been working with wireless networks for eight years, mostly close to the physical layer, and currently balances his academic work with industrial applications in the private sector. His primary focus has been on evaluating propagation modeling approaches and developing empirical solutions for wireless coverage mapping applications.

Douglas Sicker (SM'00) is the DBC Endowed Professor with the Department of Computer Science, University of Colorado, Boulder, CO, USA, with a joint appointment in, and Director of, the Interdisciplinary Telecommunications Program. He recently was the Chief Technology Officer with the National Telecommunications and Information Administration (NTIA) and the Federal Communications Commission, Washington, DC, USA. Previously, he served as Director of Global Architecture with Level 3 Communications, Inc., Broomfield, CO, USA.

Dirk Grunwald (M'89) is the Wilfred and Caroline Slade Endowed Professor with the University of Colorado, Boulder, CO, USA, in the Department of Computer Science with a dual appointment in the Department of Electrical and Computer Engineering. His research area includes networking, wireless, computer architecture, and computer systems design.

Dr. Grunwald is a member of the Association for Computing Machinery (ACM).